

INTERFEROMETRIC PERFORMANCE ASPECTS FOR TANDEM-L

Francesco De Zan

DLR - German Aerospace Center, P.O. Box 1116, D-82230 Wessling, Germany.

Email: francesco.dezan@dlr.de

ABSTRACT

DLR is studying a future L-band satellite mission (Tandem-L) in close cooperation with NASA/JPL (DES-DynI). This mission is designed to serve a variety of applications covering Solid Earth, forests, ice, etc. through the use of several SAR techniques.

We deal here with some aspects that concern Solid Earth applications and interferometry. The combination of high target coherence and the instrument large mapping capabilities calls for investigations into possible interferometric processing schemes and their associated performance.

We discuss the extent of the degradations that are introduced with respect to the theoretical bounds when only multilooked interferograms between successive images are used. Improvements can be obtained by buffering a limited number of images and interferograms, depending on the decorrelation type.

Key words: Tandem-L; interferometry; interferometric processing.

1. INTRODUCTION

Repeat-pass interferometry will play an important role in the Tandem-L mission [1, 2]. A short repeat-pass (8 days) together with a very wide swath (~ 350 km) will result in extensive mapping capabilities. We are aiming at a systematic mapping of all the most strain-affected regions of the Earth, for a total of 40 million km^2 , to be imaged with medium-high resolution (10m-20m).

To enable a 2D or 3D reconstruction of the displacements [3, 4] we want to employ ascending and descending acquisitions, and probably dedicate some time to left-looking acquisition (being the right-looking the nominal geometry).

The studies that we are conducting [5] have the goal to estimate the performance for interferometric applications based on the number of scenes that will be available, the instrument characteristics, plus models for temporal coherence and atmosphere delays .

However we have also to consider the implications that arise from the possible choices and opportunities to process the interferometric data.

2. PROCESSING ALTERNATIVES

It is clear that such a mission will produce a huge amount of data. Just for repeat-pass interferometry we currently estimate that we will have around 1 Terabyte of raw data each day. In the course of the mission, stacks of about 200 images will be generated for each targets in each line of sight. In addition these data will have a lot of interferometric potential, since the L-band coherence at 8 intervals will be high. It is then natural to pose the question of how will these data be processed.

There are probably two main ways of doing the interferometric processing for stacks of images, even though in the future they are likely to be integrated. One way is to select a few stable, isolated targets and limit the analysis to a sparse grid [6]. This is the persistent scatter approach and after the target selection the amount of data is reduced considerably. The second way is to rely on the coherence of distributed scatterers, improving the statistics by multilooking the interferograms. This approach allows for a temporal decorrelation of the scatterer [7]. The data reduction is achieved by multilooking.

However multilooking has the side effect of multiplying the number of algebraically independent interferograms, which is only $N - 1$ when no multilooking is applied. At this point it is natural to see whether some interferograms (of the $N(N - 1)/2$) are useless and can be discarded, for example on the basis of their coherence. For a stack of 200 images the number of interferograms is almost 20000.

3. SELECTION OF INTERFEROGRAMS

If we ignore geometric decorrelation (because we know it will be minor, thanks to the tight orbit control which is foreseen) and we assume that temporal decorrelation will decay monotonically (no coherence rebounds) then it seems reasonable to start using lag-1 interferograms,

i.e. the interferograms formed by each image and the following in the time series. They would be the most coherent interferograms.

The question is now how this processing will affect the final performance, compared to the optimum case where all the interferograms are processed, which is implicitly assumed in the Cramér-Rao bound [8, 7].

Even if we are using the best interferograms from the coherence point of view, it is easy to provide coherence examples where the lag-1 processing performs much worse than the optimum processing done using all the available information. These results were cross-checked with a modification of the Cramér-Rao bound and the losses can be even 6 dB [5]. The only case when we have no losses is when the coherence has a purely exponential decay (as a function of time). This is in agreement with the concept that the optimum weighting of the interferograms is given by the inverse of the true coherence matrix, which in this case is a tridiagonal matrix [9], independently of the decay velocity.

Then the issue becomes: how far deviates L-band coherence from an exponential decay? Investigations in [10] and [11] clearly suggest that the coherence decays fast in the first months but then can level off at 0.2-0.3 for the next 2-3 years (not only for desertic areas). This of course depends on the terrain type and more investigation would be needed to draw conclusions but when this happens we are in clear violation of the hypothesis of pure exponential decay. This coherence scenario is the one that opens possibilities for atmospheric phase mitigation on the time series.

Indeed the effect of atmosphere can be mitigated (filtered) when models can be employed (e.g. constant motion or at least slow in a number of acquisitions) and the coherence structure makes it possible for interferograms spanning longer times to add information to the ones spanning shorter times. In other words: averaging requires some rigidity both in the motion and in the scatterer. Either an exponentially decaying target or random walk would prevent the possibility of atmosphere mitigation.

4. SLIDING WINDOW OF IMAGES AND INTERFEROGRAMS

We will assume that the estimation process is divided in two steps, the reconstruction of the phase history (one phase for each acquisition date and for each multilooked window) and the separation of the various components (displacement, DEM errors, atmospheric delay, etc.)

The use of a sliding window of images for phase reconstruction has the advantage that the whole stack of images does not have to be loaded in memory at the same time. Actually in this way the processing could be done progressively as the images are acquired.

We investigate a scheme that would estimate the phases recursively using only submatrices of the whole interferogram matrix I_Ω and of the whole coherence matrix Γ .

In the following $\hat{\phi}^k$ indicates the estimated vector of the phases at step k . The subscripts n, m indicate a restriction to the elements from index n to index m . Here is a possible form for a recursive phase history estimation with a running windows of w images:

$$F = \left\{ \frac{1}{2} (\phi_{1,k-1}^k - \hat{\phi}_{1,k-1}^{k-1})^T \mathbf{A}_k^{-1} (\phi_{1,k-1}^k - \hat{\phi}_{1,k-1}^{k-1}) + \exp(j \phi_{k-w+1,k}^k)^H (\Gamma^{-1} \odot \mathbf{I}_\Omega)_k \exp(j \phi_{k-w+1,k}^k) \right\} \quad (1)$$

$$\hat{\phi}_{1,k}^k = \underset{\phi_{1,k}^k}{\operatorname{argmin}} F \quad (2)$$

The first term in Eq. 1 accounts for *a priori* information on the phases, which was derived in the previous steps and now is represented by the matrix A_k . The second term represents the current estimation of the phases. This would be the same as in the case of the estimation of the phases from the whole dataset [7], but the matrices involved are limited to be $w \times w$. Indeed the symbol

$$(\Gamma^{-1} \odot \mathbf{I}_\Omega)_k \quad (3)$$

has to be understood as representing the Hadamard product of two matrices, after both Γ and I_Ω have been limited to their submatrices of row and columns from $k - w + 1$ to k .

An example of the application of this recursive scheme is given in Fig. 1, where the underlying coherence is assumed constant for each interferogram pair, the worst case for lag-1 interferograms. The real phases were all set to zero, but of course no estimator is able to recover them perfectly.

Results from simulations are shown in Tab. 1, where a few different coherence scenarios are explored. It is clear that in the long-term coherence cases there is no way of attaining the Cramér-Rao limit without using some long-time interferograms.

5. FURTHER NOTES

It comes natural to ask how would be a coherence scenario in which we would have no loss when limiting ourselves to interferograms up to a certain lag. Or, similarly, how should coherences look like after a certain lag for the corresponding interferograms to be irrelevant. We already know (from the exponential decay case) that what counts is not the absolute coherence level that determine whether or not we should use an interferograms, but *the way* coherence decays.

We are looking for coherence matrices such that their inverses are band matrices, i.e. with zeros in the upper right

Table 1. Standard deviation (rad) of estimated difference between first and last phase in a series of 60 images, according to different estimation methods and for different coherence scenarios.

[rad]	lag-1 interf.	sliding window (5 images)	optimum (all interf.)
pure exponential	0.60	0.60	0.60
all time coherent	1.5	0.54	0.16
two exponentials + noise	0.55	0.38	0.25
exponential + all time coherent	0.56	0.51	0.20
exponential + noise	0.13	0.10	0.09

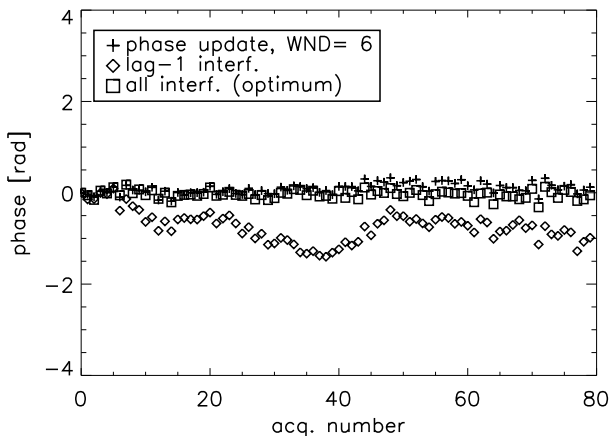


Figure 1. Example of phase history reconstruction. The coherence is 0.4 for each pair of images.

and lower left parts (once again, it is the inverse matrices that give the optimum weighting!). From a naive point of view, each element in the inverse provides an equation and we then need the same number of unknowns in the direct coherence matrix.

This looks to be an intricate problem in the general case but it becomes much easier with some additional hypotheses. We will assume to have a regular sampling of the time axis (e.g. one image every 8 days) and a stationary process for the generation of the underlying signal, so that the coherence depends only on the time span of the interferogram. The corresponding coherence matrices will be Toeplitz matrices.

In this case I propose the following conjecture: if the coherence can be modeled with an autoregressive system of order K , then the inverse will be a $2K + 1$ band matrix, which means that only interferograms up to lag K need to be considered. This would be a generalization of the exponential case.

The idea is to take an arbitrary Toeplitz coherence matrix and identify the coefficients a_n of an autoregressive model from the elements corresponding to lags

$-K, \dots, K$, using the Yule-Walker equations:

$$\gamma_k = \sum_{n=1}^K a_n \gamma_{k-n}, \quad \text{with } 1 \leq k \leq K. \quad (4)$$

With the same equations one would then predict the coherences at longer lags ($k > K$), substituting the original ones. Finally one inverts the new coherence matrix and in my numerical experiments I have always found a $2K + 1$ band matrix.

This is the case when interferograms beyond lag K don't bring any additional information.

6. CONCLUSIONS

The quantity and quality of Tandem-L data requires that we think about smart ways of exploiting them, since there is a risk that the performance will be degraded with fast processing recipes. Depending on the actual coherence scenario on the ground, we might need to process only a limited number of coherent interferograms. In case we really need to process a large number of them, we might find out that we need to do so only for a subset of the scene, for example to recover the atmospheric signature, similar to what happens for the persistent scatterers' approach.

REFERENCES

- [1] G. Krieger et al. (2009). The Tandem-L Mission Proposal: Monitoring Earth's Dynamics with High Resolution SAR Interferometry, *Proceedings of IEEE Radar Conference*.
- [2] M. Eineder et al. (2009), Scientific Requirements and Feasibility on an L-band Mission dedicated to Measure Surface Deformation, *Proceedings of IGARSS 2009*, pp. 1–4, [to be published]
- [3] T. J. Wright et al. (2004), Toward mapping surface deformation in three dimensions using InSAR, *Geophysical Research Letters*, vol. 31, pp. L01607.1–L01607.5.

- [4] F. Rocca (2004), 3D motion recovery with multi-angle and/or left right interferometry, *Proc. of Fringe 2003 Workshop*, pp. 1–5.
- [5] F. De Zan et al. (2009), Mission design and performance for systematic deformation measurements with a spaceborne SAR system, *Proceedings of IGARSS 2009*, pp. 1–4, [to be published]
- [6] A. Ferretti et al. (2001), Permanent scatterers in SAR interferometry. *IEEE Trans. Geosci. and Remote Sensing*, vol. 39 , pp. 8–20
- [7] A. Monti Guarnieri and S. Tebaldini (2008), On the exploitation of target statistics for SAR interferometry applications, *IEEE Trans. Geosci. Remote Sensing*, vol. 46, pp. 3436–3443.
- [8] A. Monti Guarnieri and S. Tebaldini (2007), Hybrid Cramér-Rao bound for crustal displacement field estimators in SAR interferometry, *IEEE Signal Proc. Letters*, vol. 14, pp. 1012–1015.
- [9] A. Ferretti et al. (2008), Moving from PS to Slowly Decorrelating Targets: A Prospective View, *Proceeding of EUSAR 2008*, pp. 1–3
- [10] M. Shimada et al. (2005), The polarimetric and interferometric potential of ALOS PALSAR *Proc. of POLinSAR 2005 Workshop*, pp. 1–6.
- [11] A. Parizzi et al. (2009), First Results from Multi-frequency Interferometry - A comparison of different Decorrelation Time Constants at X, C and L-band, at Fringe 2009 Workshop